

# Fidelity susceptibilities in the one-dimensional extended Hubbard model

Wing Chi Yu and Shi-Jian Gu\*

*Department of Physics and ITP, The Chinese University of Hong Kong, Hong Kong, China*

Hai-Qing Lin

*Beijing Computational Science Research Center, Beijing 100084, China*

(Dated: September 12, 2021)

We investigated the fidelity susceptibility in the one-dimension (1D) Hubbard model and the extended Hubbard model at half-filling via the density matrix renormalization group. From the numerical results, we argue that in the 1D Hubbard model, the fidelity susceptibility shows a divergence at two points which is infinitesimally close to the critical point while it is always extensive exactly at the critical point. For the extended Hubbard model, we found that for a properly chosen driving parameter, the fidelity susceptibility is able to reveal the quantum phase transitions between the PS (phase separation)-superconducting, superconducting-CDW (charge-density wave), CDW-SDW (spin-density wave), SDW-PS, CDW-BOW (bond-order wave), and the BOW-SDW phases.

PACS numbers: 05.30.Rt, 03.67.-a, 64.70.Tg, 71.10.Fd

## I. INTRODUCTION

At absolute zero temperature, being driven by the quantum fluctuation rooted from the Heisenberg uncertainty principle, a many-body system can undergo a quantum phase transition (QPT) [1] when it is tuned across some external parameters like magnetic field. Across the transition point, the ground state wavefunction of the system exhibits an abrupt change in the qualitative structure. The ground state fidelity, which is a concept from quantum information science to quantify the similarity between two states, is expected to show a sudden drop at the critical point. With this primary motivation, people started to explore the role of fidelity played in QPTs [2, 3]. The significance of the fidelity to witness a QPT has been testified in a large variety of models including the Dicke model [3], 1D XY model in a transverse field [3], quadratic fermion Hamiltonians [4, 5], and Bose-Hubbard model [6, 7] (For a review, please refer to Ref. [8]).

Along the streamline of fidelity, the fidelity susceptibility [9, 10] was proposed. The fidelity susceptibility is the leading response of the fidelity to the external perturbation. It has been found to be related to the correlation function of the driving term in the Hamiltonian [9]. Basing on this general relation, a scaling relation between the size dependence of the fidelity susceptibility, the dynamic exponent, and the scaling dimension of the driving term was also obtained through scaling transformation [11, 12]. These suggest that the fidelity susceptibility could be a potential candidate to witness the Landau type QPTs through its divergence at the critical point. As a pure Hilbert space geometrical quantity, the application of the fidelity and fidelity susceptibility does not require any a priori knowledge in the system's symmetry

and this make it advantageous to the study of QPTs. This approach has also been successfully applied to detect the topological QPT, which fall beyond the framework of the spontaneous symmetry-breaking theory, in the 2D Kitaev model on a honeycomb lattice [13]. Recently, a equality relating the fidelity susceptibility and the spectral function was also derived [14]. This makes the fidelity susceptibility directly measurable in experiments via neutron scattering or the angle-resolved photoemission spectroscopy (ARPES) techniques.

However, the ability of the fidelity susceptibility to detect for Beresinskii-Kosterlitz-Thouless (BKT) transitions [15–17] is still controversial. For examples, while the fidelity susceptibility was found to be divergent at the BKT quantum critical point of the 1D spin-half XXZ model [18–20], no singularity was found when crossing the BKT transition point of the 1D asymmetric Hubbard model [12]. To investigate the ability of the fidelity susceptibility to witness a BKT transition, in particular in the 1D Hubbard and extended Hubbard model at half-filling, is the motivation of this work.

The fidelity susceptibility in the 1D Hubbard model has been investigated separately by two groups [9, 21]. You *et. al.* showed that the normalized fidelity susceptibility at the critical point is a constant even when the system size is very large [9]. On the other hand, using Bosonization technique with the aid of exact diagonalization, Venuti *et. al.* argued that the normalized fidelity susceptibility diverges in the thermodynamic limit when one approaches the critical point on the half-filling line [21]. There is still no an agreement on whether the fidelity susceptibility is able to signal for the BKT transition in the model. In this work, we use the density matrix renormalization group (DMRG) approach to calculate the fidelity susceptibility in the model and performed a detail scaling analysis. With the supplement of analytic calculation, we argued that the fidelity susceptibility diverges at some infinitesimal distance away from the critical point in the thermodynamic limit.

---

\*Email: sjgu@phy.cuhk.edu.hk

We also studied the fidelity susceptibility in the 1D extended Hubbard model at half-filling. The model exhibits a very rich ground state phase diagram consisting of the charge-density wave (CDW), spin-density wave (SDW), phase separation (PS), singlet-superconducting (SS), triplet-superconducting (TS) and bond-order wave (BOW) phases. To the best of our knowledge, there is no investigation on the fidelity susceptibility in the model available so far. Using DMRG simulation, we investigate the ability of the fidelity susceptibility in clarifying the ground state phase diagram of the model. We found that the phase boundaries, except the SS-TS one, can be roughly revealed by the fidelity susceptibility with properly chosen driving parameters. Our finding may provide an alternate way to study the controversies in the model's ground state phase diagram [22–24].

The paper is organized as follows: In section II, the mathematical formulation of the fidelity susceptibility is reviewed. Then the analysis of the fidelity susceptibility in the 1D Hubbard model and the extended Hubbard model is presented in section III and IV respectively. Finally, a conclusion is given in section V.

## II. FIDELITY SUSCEPTIBILITY

Consider a many-body system, the Hamiltonian can be generally written as

$$H(\lambda) = H_0 + \lambda H_I, \quad (1)$$

where  $\lambda$  is the external driving parameter and  $H_I$  is the driving Hamiltonian. Denoting the eigenstates and eigenenergies as  $|\Psi_n\rangle$  and  $E_n$  respectively such that  $H(\lambda)|\Psi_n(\lambda)\rangle = E_n(\lambda)|\Psi_n(\lambda)\rangle$ . The ground state fidelity of a pure state is defined as [3]

$$F(\lambda, \lambda + \delta\lambda) = |\langle\Psi_0(\lambda)|\Psi_0(\lambda + \delta\lambda)\rangle|, \quad (2)$$

which measures the overlap between the two ground states at a different  $\lambda$ . Geometrically, the fidelity represents the angular distance between the two ground states differed by a small value of the driving parameter  $\delta\lambda$  in the Hilbert space. It has a range between 0 and 1. If the two states are the same up to a phase factor, the fidelity is equal to one. If the states are orthogonal, the fidelity becomes zero. Across a quantum critical point, the fidelity is expected to exhibit a significant drop as the ground states on the two sides of the critical point has qualitatively different structures.

For a phase transition which is not induced by the ground state level-crossing, the ground state of the system is non-degenerated in a finite system. Consider the system's parameter varies from  $\lambda$  to  $\lambda + \delta\lambda$ , one can apply the non-degenerated perturbation theory by treating  $\delta\lambda H_I$  as a perturbation. To the first order correction of the ground state, we have

$$|\Psi_0(\lambda + \delta\lambda)\rangle = |\Psi_0(\lambda)\rangle + \delta\lambda \sum_{n \neq 0} \frac{H_I^{n0}(\lambda)|\Psi_n(\lambda)\rangle}{E_0(\lambda) - E_n(\lambda)}, \quad (3)$$

where

$$H_I^{n0} = \langle\Psi_n(\lambda)|H_I|\Psi_0(\lambda)\rangle. \quad (4)$$

Together with the normalization condition, the fidelity in Eq. (2) to the lowest order of  $\delta\lambda$  can be expressed as

$$F(\lambda, \lambda + \delta\lambda) \simeq 1 - \frac{1}{2}(\delta\lambda)^2 \sum_{n \neq 0} \frac{H_I^{n0}H_I^{0n}}{(E_0(\lambda) - E_n(\lambda))^2}. \quad (5)$$

Recall that the maximum of the fidelity is equal to one at  $\delta\lambda = 0$ . It is an even function of  $\delta\lambda$  and the first order correction to the fidelity should be zero as expected. The second order term, which is the leading response of the fidelity to the external perturbation, is defined as the fidelity susceptibility [3, 9]

$$\chi_F(\lambda) \equiv \lim_{\delta\lambda \rightarrow 0} \frac{-2 \ln F}{(\delta\lambda)^2}, \quad (6)$$

$$= -\frac{\partial^2 F}{\partial(\delta\lambda)^2}. \quad (7)$$

From Eq. (5), the perturbation form of the fidelity susceptibility is given by

$$\chi_F(\lambda) = \sum_{n \neq 0} \frac{|\langle\Psi_n(\lambda)|H_I|\Psi_0(\lambda)\rangle|^2}{(E_0(\lambda) - E_n(\lambda))^2}. \quad (8)$$

One may realize that the form of the fidelity susceptibility is very similar to that of the second derivative of the ground state energy with respect to  $\lambda$ , i.e.

$$\frac{\partial^2 E_0(\lambda)}{\partial\lambda^2} = \sum_{n \neq 0} \frac{2|\langle\Psi_n(\lambda)|H_I|\Psi_0(\lambda)\rangle|^2}{E_0(\lambda) - E_n(\lambda)}. \quad (9)$$

The main difference is in the exponent of the denominator. Therefore, one may expect that both the divergence of the fidelity susceptibility and the second derivative of the ground state energy at the critical point is intrinsically due to the vanishing of the energy gap in the thermodynamic limit [25]. However, the difference in the exponent suggests that the fidelity susceptibility is a more sensitive seeker and may be able to detect higher order quantum phase transitions.

## III. ANALYSIS ON THE ONE-DIMENSIONAL HUBBARD MODEL

The Hubbard model is the simplest model in condensed matter physics that captures the electron-electron correlation in solids. It was first proposed independently by Martin Gutzwiller[26], Junjiro Kanamori[27] and, of course, John Hubbard[28] in 1963, and is put forward by Hubbard's sequential works [29–33]. Originally, the model was proposed to study the itinerant ferromagnetism in transition metals such as iron and nickel. However, its application was later found to be far beyond this.

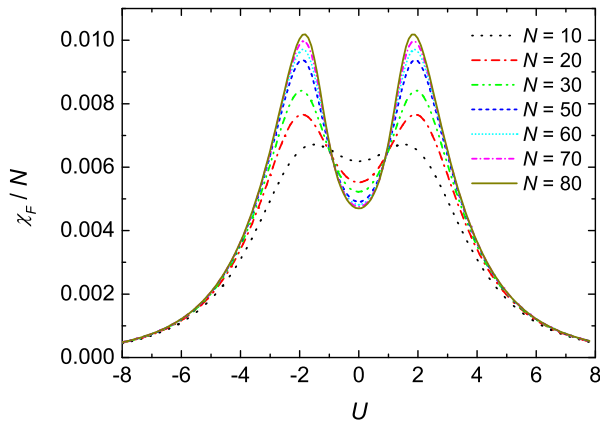


FIG. 1: The normalized fidelity susceptibility as a function of  $U$  with various system size  $N$  in the 1D Hubbard model at half-filling. The fidelity susceptibility shows two peaks around  $U = 0$  while it exhibits a local minimum at  $U = 0$ .

For examples, the model has also used in attempts to describe high- $T_c$  superconductivity. Recently with advance in cold atom experiments, the model was also successfully realized by ultracold Fermi gas in optical lattices [34, 35].

The Hamiltonian of the model is given by

$$H_{\text{HM}} = -t \sum_{j=1, \sigma} \left( c_{j, \sigma}^\dagger c_{j+1, \sigma} + h.c. \right) + U \sum_{j=1} n_{j, \uparrow} n_{j, \downarrow} \quad (10)$$

where  $c_{j, \sigma}^\dagger$  and  $c_{j, \sigma}$  ( $\sigma = \uparrow, \downarrow$ ) is respectively the creation and annihilation operators of an electron with a spin  $\sigma$  at the site  $j$  and they satisfies the usual anti-commutation relations of fermion operators.  $n_{j, \sigma} = c_{j, \sigma}^\dagger c_{j, \sigma}$  is the number operator of electrons with spin  $\sigma$  at site  $j$ .  $t$  is the hopping amplitude of electrons between nearest neighboring sites and is taken as one in the our analysis for convenience.  $U$  is the strength of the on-site interaction. Originally, the  $U$  term was introduced to describe the repulsive Coulomb interaction of the electrons. One may expect only to consider positive values of  $U$ . However, in some materials with interactions like the electron-phonon or the excitonic ones,  $U$  can have an effective negative value. Without loss of generality, we will consider the whole range of values of  $U$ . In the case of half-filling, the model exhibits a BKT transition at  $U = 0$  and the system transits from a metallic phase to a Mott-insulating phase as  $U$  changes from negative to positive.

Treating the  $U$  term as the driving Hamiltonian, i.e.

$$H_I = \sum_{j=1}^N n_{j, \uparrow} n_{j, \downarrow} = \sum_{j=1}^N c_{j, \uparrow}^\dagger c_{j, \uparrow} c_{j, \downarrow}^\dagger c_{j, \downarrow}, \quad (11)$$

the fidelity susceptibility is calculated by DMRG simulation for system sizes  $N = 10$  to  $N = 90$  with open boundary conditions. The maximum number of block states kept is  $m = 600$ . Fig. 1 shows a plot of the normalized fidelity susceptibility as a function of the driving

parameter  $U$ . The fidelity susceptibility is a local minimum at the critical point  $U_c = 0$  and attain two maxima at some values of  $U = U_{\text{max}}$  away from the critical point.

At the point  $U = 0$ , the model is reduced to the tight-binding model and analytical solution for the fidelity susceptibility can be obtained. For open boundary conditions, the Fourier transformation on the fermion operators is given by

$$c_j^\dagger = \sqrt{\frac{2}{N+1}} \sum_k \sin(kj) c_k^\dagger, \quad (12)$$

$$c_j = \sqrt{\frac{2}{N+1}} \sum_k \sin(kj) c_k, \quad (13)$$

where  $k = n\pi/(N+1)$ , and  $n = 1, 2, \dots, N$ . The driving Hamiltonian in Eq. (11) becomes

$$H_I = \frac{1}{2(N+1)} \sum_{k_1, k_2, k_3, k_4} \tilde{\delta} c_{k_1, \uparrow}^\dagger c_{k_2, \uparrow} c_{k_3, \downarrow}^\dagger c_{k_4, \downarrow}. \quad (14)$$

where

$$\begin{aligned} \tilde{\delta} \equiv & \delta_{k_1 - k_2 - k_3 + k_4, 0} + \delta_{k_1 - k_2 + k_3 - k_4, 0} \\ & - \delta_{k_1 - k_2 - k_3 - k_4, 0} - \delta_{k_1 - k_2 + k_3 + k_4, 0} \\ & - \delta_{k_1 + k_2 - k_3 + k_4, 0} - \delta_{k_1 + k_2 + k_3 - k_4, 0} \\ & + \delta_{k_1 + k_2 - k_3 - k_4, 0} + \delta_{k_1 + k_2 + k_3 + k_4, 0}, \end{aligned} \quad (15)$$

and  $\delta$  is the Kronecker delta. The ground state is given by electrons filling up to the Fermi level and the fidelity susceptibility is contributed by the scattering of electrons below the Fermi level to above the Fermi level. With Eq. (8) and (14), the fidelity susceptibility can be calculated as

$$\chi_F = \frac{1}{4(N+1)^2} \sum_{\substack{k_1, k_3 > k_F \\ k_2, k_4 \leq k_F}} \frac{\tilde{\delta}^2}{(\Delta E)^2}, \quad (16)$$

where  $k_F$  is the Fermi wavevector and

$$\Delta E = -2(\cos k_1 + \cos k_3 - \cos k_2 - \cos k_4). \quad (17)$$

With these expressions, we can obtain the fidelity susceptibility by carrying out the sum numerically.

Figure 2 shows a plot of the fidelity susceptibility as a function of  $N$  up to a system size of 2502. From the figure, one can observe that the fidelity susceptibility is linear in  $N$  for a large enough system. From the slope of the straight line, we obtained

$$\chi_F(U=0) = 0.05 + 0.0042N. \quad (18)$$

So in the thermodynamic limit,  $\chi_F/N$  at  $U = 0$  converges to a constant value of  $0.0042 \pm 10^{-7}$ .

Furthermore, the normalized fidelity susceptibility at  $U = 0$  obtained from DMRG is compared with the analytic result in Fig. 3. The data agrees well with each other. The maximum discrepancy of the DMRG data

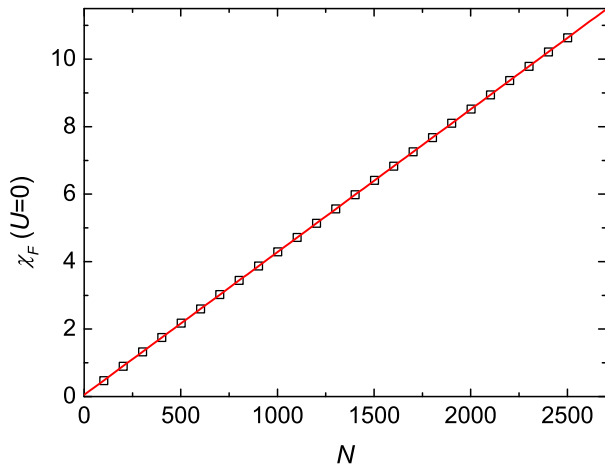


FIG. 2: The analytical result of the fidelity susceptibility at  $U = 0$  in Eq. (16) as a function of  $N$  in the 1D Hubbard model. The straight line shows a linear fitting of the data points.

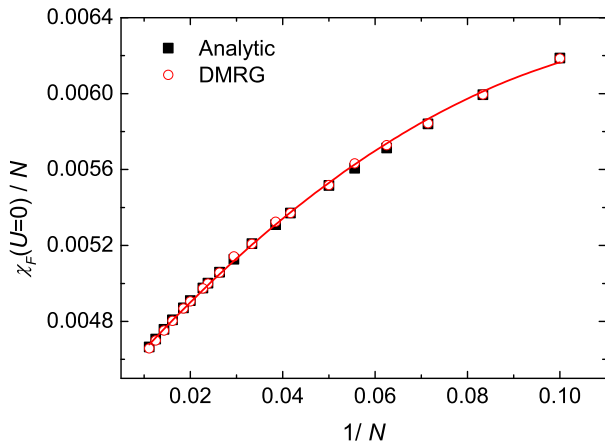


FIG. 3: The fidelity susceptibility at  $U = 0$  of the 1D Hubbard model as a function of  $1/N$ . The open and solid symbol represents data obtained from DMRG and the analytical expression in Eq. (16) respectively. The curve shows the second order polynomial fitting on the DMRG data.

from the analytic one is about 0.5%. We may reasonably trust our DMRG result when doing the analysis.

From the quadratic fitting of the DMRG data in Fig. 3, we have

$$\frac{\chi_F(U=0)}{N} = 0.00438 + 0.0283\frac{1}{N} - 0.104\frac{1}{N^2}. \quad (19)$$

In the thermodynamic limit,  $\chi_F(U=0)/N \rightarrow 0.00438 \pm 0.00001$ , which is consistent with the analytical result to one significant figure.

Next, let's investigate the scaling behavior of the two peaks away from the critical point. They are symmetric about the  $U = 0$  axis. So we can only pick one of the peaks to do the finite size scaling analysis. The maximum value of the normalized fidelity susceptibility is plotted

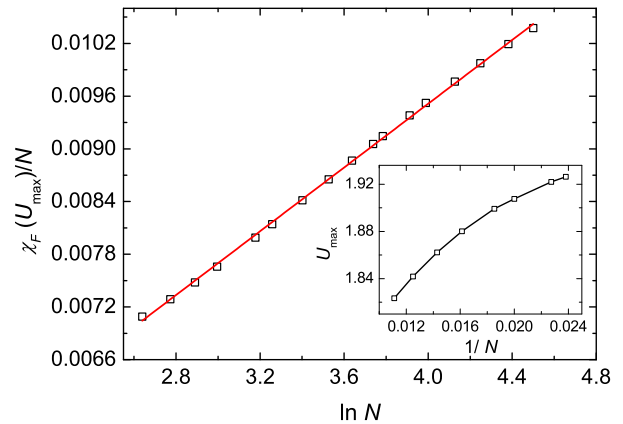


FIG. 4: The maximum of the normalized fidelity susceptibility of the 1D Hubbard model as a function of  $\ln N$ . The straight line shows the linear fitting of the data points. Inset shows a plot of  $U_{\max}$  at which the maximum of fidelity susceptibility occurs as a function of  $1/N$ .

as a function of  $\ln N$  in Fig. 4. The data points falls on a straight line. From linear fitting, we have

$$\frac{\chi_F(U_{\max})}{N} \sim \ln N. \quad (20)$$

In the thermodynamic limit, the normalized fidelity susceptibility shows a logarithmic divergence.

The inset of figure 4 shows the scaling behavior of the value of  $U$  at which the maximum of the fidelity susceptibility takes place. We see that as the system size increases,  $U_{\max}$  decreases. In the thermodynamic limit, we expect it to tend to a point which is infinitesimally close to zero.

Integrating the above analyses, we argue that in the thermodynamic limit, the fidelity susceptibility is expected to show a logarithmic divergence at two points  $0^+$  and  $0^-$  which is infinitesimally close to the true critical point  $U = 0$ . Exactly at the critical point, the normalized fidelity susceptibility is always a local minimum and have a constant value of 0.004. We try to understand this phenomena by noting that the ground state of the system is a charge-density wave (CDW) and a spin-density wave (SDW) on the sides of negative and positive  $U$  respectively. However, at the critical point  $U = 0$ , the system is a free electron system which is completely different from a CDW or a SDW. This point may be considered as another phase. So as  $U$  is tuned from  $-\infty$  to  $+\infty$ , the ground state of the system undergoes two abrupt changes, one from CDW to a free electrons and the other time from free electrons to SDW. This gives rise to the two peaks in the fidelity susceptibility. For the fidelity susceptibility to be continuous in finite systems, it must experience a local minimum in between. As the two peaks have to be symmetric as a result of particle-hole symmetry in the model, the local minimum has to occur at  $U = 0$ .

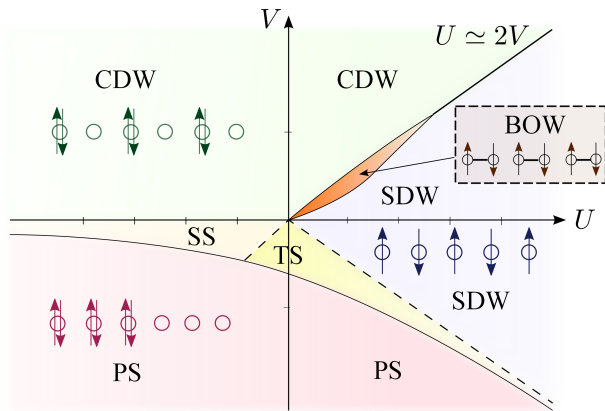


FIG. 5: A schematic drawing of the ground state phase diagram of the 1D extended Hubbard model at half-filling.

#### IV. ANALYSIS ON THE ONE-DIMENSIONAL EXTENDED HUBBARD MODEL

Despite the historical importance of the Hubbard model, it is limited to describe materials in which long-ranged Coulomb interaction plays an essential role. Examples included organic conductors such as TTF-TCNQ [36, 37] and  $\pi$ -conjugated polymers like polydiacetylene [38]. To model these materials, it is necessary to invoke at least the nearest-neighbor Coulomb interaction. This leads to the extended Hubbard model described by the Hamiltonian

$$H_{\text{EHM}} = -t \sum_{j=1,\sigma} \left( c_{j,\sigma}^\dagger c_{j+1,\sigma} + h.c. \right) + U \sum_{j=1} n_{j,\uparrow} n_{j,\downarrow} + V \sum_{j=1} n_j n_{j+1}, \quad (21)$$

where  $n_j = n_{j,\uparrow} + n_{j,\downarrow}$ . The  $V$  term in the Hamiltonian captures the nearest-neighbor interaction and it contributes whenever two neighboring sites are simultaneously occupied.

In the past few decades, a variety of technique was implanted to study the ground state phase diagram of the model. It was found that the model exhibits a very rich phase diagram (See Fig. 5). In the strong coupling limit ( $|U|, |V| \gg t$ ), perturbation analysis suggested the existence of charge-density wave (CDW), the spin-density wave (SDW) and phase separation (PS) phases in the ground state phase diagram [39–41]. In the weak coupling limit ( $|U|, |V| \ll t$ ), analytic studied through the g-ology [42–44] and bosonization method [45, 46] in the past also gave some insight on the ground state phase diagram of the model. By investigating various correlation functions in a given region, these theories predicted the existence of the CDW, the SDW, singlet superconducting (SS) and the triplet superconducting (TS) phase.

Although much effort has been devoted to study the extended Hubbard model in the past, there remain controversies in its ground state phase diagram. For positive

$U$  and  $V$ , while the strong coupling theories predicted the CDW-SDW phase transition to be first order, the weak coupling theories tell that it is continuous. By studying the excitation spectra with numerical exact diagonalization, Nakamura pointed out that there also exist a spontaneous dimerized phase, the bond-order wave (BOW) phase, in a narrow region between the SDW phase and the CDW phase up to a tricritical point [22]. On the other hand, Jeckelmann argued that the BOW phase only exists on a short segment of the critical line, rather than a stripe, of the CDW-SDW transition from DMRG studies [23, 24]. Subsequent efforts using quantum Monte Carlo stimulation [47, 48], density matrix renormalization group [49, 50], and analytical methods [51, 52] have been devoted to clarify this issue in the ground state phase diagram. Recently, the concept from quantum information science, namely the entanglement entropy, was also used to explore the problem [53, 54]. Although most of the studies confirmed the existence of the BOW phase, the shape of it and the position of the tricritical point still have not settled into agreement.

In the following, let's take  $t = 1$  again for convenience and consider the case of half-filling. Unless otherwise specified, the data presented are obtained from DMRG with open boundary conditions. The fidelity susceptibility depends on the path of the driving Hamiltonian. In our analysis, we considered taking the  $U$  term and the  $V$  term as the driving Hamiltonian respectively. Note that one can also consider the case of varying both  $U$  and  $V$  together, but we will not discuss it here.

##### A. $U$ as the driving parameter

The driving Hamiltonian is taken as

$$H_I = \sum_{j=1}^N n_{j,\uparrow} n_{j,\downarrow}. \quad (22)$$

To have a brief picture of the overall phase diagram, we first carried out numerical exact diagonalization to calculate the fidelity susceptibility for a small system, i.e.  $N = 10$ . To minimize the size effect, we used periodic boundary conditions in the calculation.

Figure 6 shows a 3D plot of the fidelity susceptibility as a function of  $U$  and  $V$ , and also the contour on the  $U$ - $V$  plane. From the figure, we can observe that, even with such a small system size, the fidelity susceptibility has captured the phase boundaries of the CDW-SDW, SDW-PS, PS-CDW transitions. In the negative value of  $V$ , the fidelity susceptibility shows a very sharp peak at the phase boundary between the PS and SDW phase. The huge peak there may be understood by the fact that the transition is a first order transition. The transition is caused by a level-crossing between the ground state and the excited state in the energy spectrum. The crossing occurs even in a very small system. So the fidelity as a measure of the overlap between the ground state differed

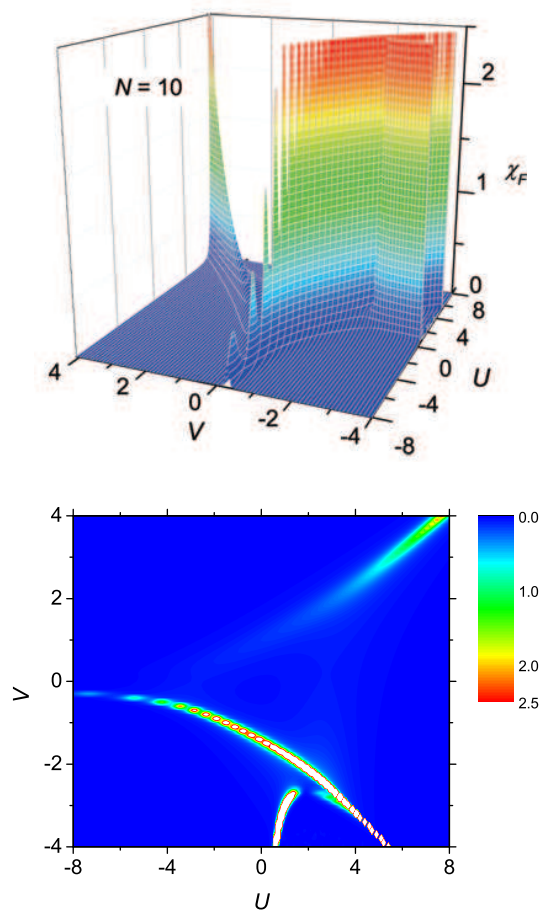


FIG. 6: (Top) A 3D plot of the fidelity susceptibility as a function of  $U$  and  $V$  in the 1D extended Hubbard model. (Bottom) A contour of the 3D plot on the  $U$ - $V$  plane.  $U$  is treated as the driving parameter in this case. The data is obtained from numerical exact diagonalization for  $N = 10$  with periodic boundary conditions.

by a small  $U$  should have a sharp drop at the critical point. This drop in fidelity is then reflected in the peak of the fidelity susceptibility.

Moreover, in the contour plot, there is also another sharp boundary in the PS phase in the positive  $U$  and negative  $V$  regime (The boundary going through the point  $U \simeq 0.6$  and  $V = -4$ ). However, this is not a true critical line. It is just a finite size effect. Consider a PS state

$$\text{PS(a): } \uparrow\downarrow \uparrow\downarrow \uparrow\downarrow \uparrow\downarrow \uparrow\downarrow \uparrow\downarrow \uparrow\downarrow \uparrow\downarrow 0 \ 0 \ 0 \ 0 \ 0 \ 0, \quad (23)$$

having energy  $(2N - 4)V + NU/2$ . The ground state in the  $U, V \rightarrow -\infty$  limit is a superposition of the above state and its translational symmetric states. Now if  $U$  increases and gradually becomes positive (but still not reaching the SDW phase), the on-site interaction term would like to break the electron pairs and one doubly occupied site tends to be singly occupied. The weight of

$$\text{PS(b): } 0 \ 0 \ \uparrow \uparrow\downarrow \uparrow\downarrow \uparrow\downarrow \uparrow\downarrow \uparrow\downarrow \downarrow \ 0 \ 0 \quad (24)$$

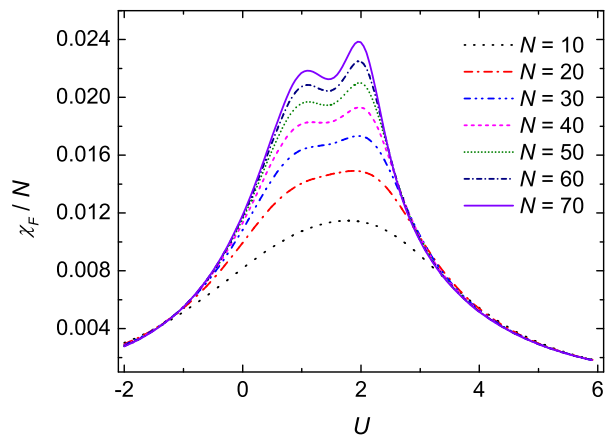


FIG. 7: The normalized fidelity susceptibility as a function of  $U$  in the 1D extended Hubbard model at half-filling for  $V = 1$ .

increases and at some positive value of  $U$ , PS(b) would become the dominate configuration in the ground state. The peaks in the fidelity susceptibility is in fact correspond to the crossover between the two PS states. Note that the configuration in PS(b) has an energy of  $(2N - 4)V + (N/2 - 1)U$ . The energy difference between the PS(a) and PS(b) configuration is  $U$  and this difference becomes negligible when  $N$  is large. So the crossover peak in the fidelity susceptibility would be suppressed in the thermodynamic limit.

For the case of positive  $U$  and  $V$ , the contour in Fig. 6 also reveals the SDW-CDW phase transition. The peaks in the fidelity susceptibility are stronger in the large  $U$  and  $V$  regime than in the small  $U$  and  $V$  region. This is because the phase transition there is a discontinuous one. For the weak and intermediate coupling regime, the phase boundary and its detail, for examples the BOW phase, is merely resolved. The transition here is believed to be continuous for the CDW-BOW and BKT for the BOW-SDW transition. It would thus expected to be harder to realize in a small system. To have a more detail clarification of the phase diagram, we calculated the fidelity susceptibility for a larger system size using DMRG. Two particular paths, varying  $U$  while fixing  $V = 1$  and  $V = -0.5$  respectively, will be discussed in the following.

#### 1. Case I: $V=1$

Figure 7 shows a plot of the normalized fidelity susceptibility as a function of the driving parameter  $U$ . For system size smaller than 40, there is only one maximum occurs around  $U = 2$ . However, as the system size increases, there is another local maximum build up around  $U = 1$ . While  $\chi_F/N$  is intensive away from the critical region, the two local maxima in the vicinity of the critical point become larger and larger as the system gets bigger. We can reasonably suspect that the maximum around  $U_{\max 1} \simeq 1$  and  $U_{\max 2} \simeq 2$  is corresponding to

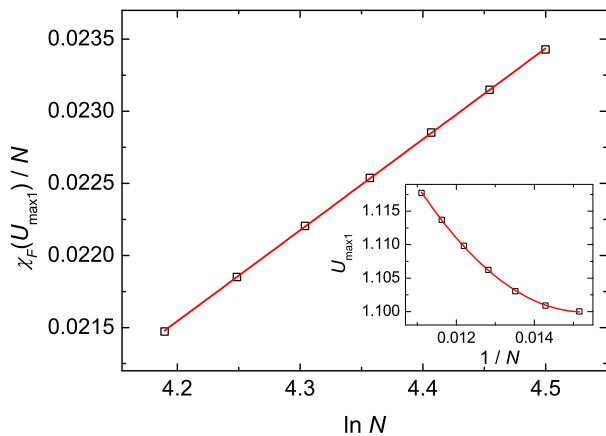


FIG. 8: A semi-ln plot of the maximum of the fidelity susceptibility around  $U_{\max 1} \simeq 1$  as a function of the system size in the 1D extended Hubbard model at half-filling. Here  $V = 1$  and  $U$  is taken as the driving parameter. The straight line shows the linear fitting of the data point. The inset shows a plot of  $U_{\max 1}$  as a function of  $1/N$  and the curve shows a second order polynomial fitting of the data.

the SDW-BOW and BOW-CDW transition respectively.

In Fig. 8, the maximum of the fidelity susceptibility at  $U_{\max 1}$  is plotted against  $\ln N$ . The data points fall perfectly onto a straight line. We have

$$\frac{\chi_F(U_{\max 1})}{N} \sim \ln N. \quad (25)$$

The inset of figure 8 shows a plot of the value of  $U_{\max 1}$  as a function of  $1/N$ . The data points are fitted by a second order polynomial curve. From the fitting, we found that

$$\lim_{N \rightarrow \infty} U_{\max 1} = 1.340 \pm 0.004. \quad (26)$$

For the maximum at  $U_{\max 2}$ , the scaling behavior of the fidelity susceptibility is shown in Fig. 9. The normalized fidelity susceptibility as a function of  $N$  is plotted in a natural logarithmic scale in the figure. We can see that the normalized fidelity susceptibility scales algebraically with the system size. From linear fitting, we obtained

$$\frac{\chi_F(U_{\max 2})}{N} \sim N^{0.3784 \pm 0.0001}. \quad (27)$$

Moreover, the value of  $U_{\max 2}$  is plotted as a function of  $1/N$  in the inset of Fig. 9. As the system size increases,  $U_{\max 2}$  tends to decrease. The data points are well fitted onto a quadratic curve. We obtained, in the thermodynamic limit,

$$\lim_{N \rightarrow \infty} U_{\max 2} = 1.842 \pm 0.002. \quad (28)$$

From the above analysis, we argue that the fidelity susceptibility diverges at two values of  $U$ , which indeed

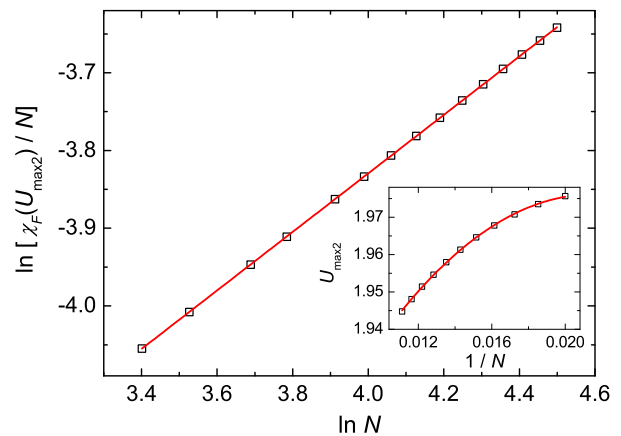


FIG. 9: A ln-ln plot of the maximum of the fidelity susceptibility around  $U = 2$  as a function of the system size in the 1D extended Hubbard model at half-filling. Here  $V = 1$  and  $U$  is taken as the driving parameter. The straight line, which shows the linear fitting of the data point, has a slope of  $0.3784 \pm 0.0001$ . Inset shows a plot of  $U_{\max 2}$  as a function of  $1/N$ . The curve shows a second order polynomial fitting of the data points.

corresponds to the SDW-BOW and BOW-CDW transition respectively. While in the former case the divergence is logarithmic, the fidelity susceptibility diverges algebraically in the latter case. In the thermodynamic limit, the two critical points tends to a different value in Eq. (26) and (28). So instead of just a line segment, we tend to believe that the BOW phase is a stripe in the ground state phase diagram on the  $U - V$  plane. At  $V = 1$ , the width of the BOW phase is found to be

$$\Delta U_{\text{BOW}} = 0.502 \pm 0.006. \quad (29)$$

This width obtained agrees roughly with the analytical result obtained from g-ology in Ref. [51]. However, the critical points obtained in Eq. (26) and (28) deviate from those obtained by calculating the correlation functions [49] or the spin and the charge gaps in other studies [48, 50]. We are not sure the apparent agreement in  $\Delta U_{\text{BOW}}$  with the g-ology result is just a coincidence or there are more physics to be explored.

## 2. Case II: $V = -0.5$

Next, let's consider the path along  $V = -0.5$ . In this case, the system goes through the PS, SS, TS, and the SDW phase as  $U$  increases. Fig. 10 shows a plot of the fidelity susceptibility as a function of  $U$  for various system sizes. Here we have only shown the result for  $U \gtrsim -3$ . For the data with  $U$  smaller than this value, the fidelity susceptibility is strongly fluctuating with large amplitudes and becomes unreliable. This is a result of symmetry breaking in the simulation. In principle, the ground state is given by a superposition of PS(a) and its

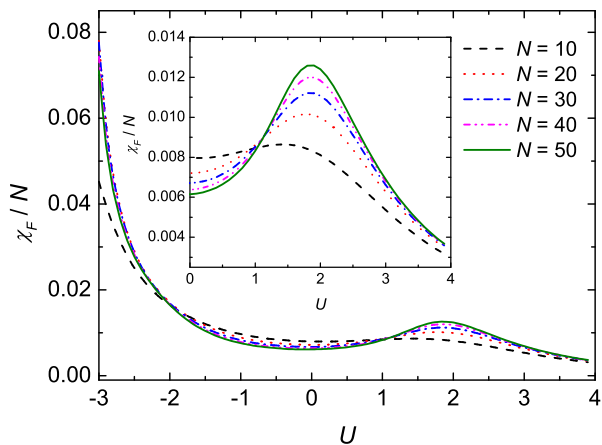


FIG. 10: The fidelity susceptibility as a function of  $U$  in the 1D extend Hubbard model at half-filling for  $V = -0.5$ . The inset shows a close-up of the fidelity susceptibility around  $U = 0$  to  $U = 4$ .

translational symmetric states for a finite system. However, the potential barrier between these translational invariant state for PS(a) state is very large especially in a large system. If we start with a random initial wavefunction in the stimulation, the system would converge to one of the translational invariant states and leads to a strongly fluctuating fidelity susceptibility. Nevertheless, though the critical point cannot be exactly located, we can still notice the PS-SS phase transition when the fidelity susceptibility changes from a fluctuating pattern into a smooth function.

In Fig. 10, one can also observe a small peak in the fidelity susceptibility around  $U \simeq 2$ . This peak indeed indicate the transition from the superconducting phase to the SDW phase of the model. From the inset, we can see that  $\chi_F/N$  shows a non-trivial size dependence. This local maximum of the normalized fidelity susceptibility is plotted as a function of  $\ln N$  in Fig. 11. The data points agrees well with the linear fitted line. So we have

$$\frac{\chi_F(U_{\max})}{N} \sim \ln N, \quad (30)$$

and it diverges in the thermodynamic limit.

To determine the location of  $U_{\max}$  in the thermodynamic limit, we plotted the value of it as a function of  $1/N$  in the inset of Fig. 11. From the second order polynomial fitting, we have obtained

$$\lim_{N \rightarrow \infty} U_{\max} = 1.70 \pm 0.03. \quad (31)$$

For the SS-TS transition, we were not able to observe any significant peaks in the fidelity susceptibility around the transition point. This may due to the limitation in the small system sizes being stimulated. Another difficulty may arise from the narrow width of the superconducting phase for  $V = -0.5$  in the phase diagram. Together with the effect of the strong peak from PS-SS transition, the SS-TS transition peak may be suppressed.

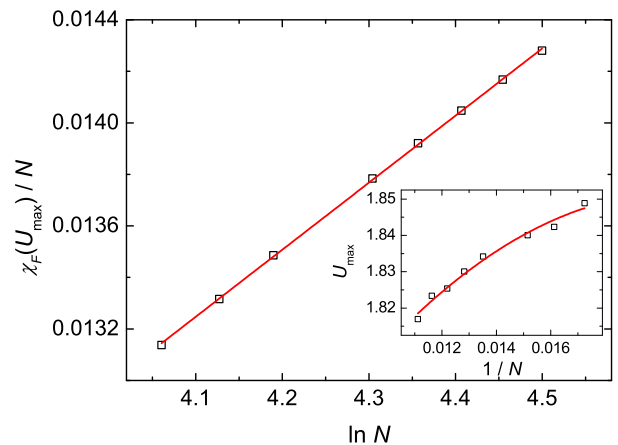


FIG. 11: A semi-ln plot of the maximum of the fidelity susceptibility as a function of the system size in the 1D extended Hubbard model at half-filling. Here  $V = -0.5$  and  $U$  is taken as the driving parameter. The straight line is a linear fitting of the data points. Inset shows a plot of  $U_{\max}$  as a function of  $1/N$  in the 1D extended Hubbard model at half-filling for  $V = -0.5$ . The curve shows a second order polynomial fitting of the data points.

## B. $V$ as the driving parameter

Next we consider the  $V$  term as the driving Hamiltonian, i.e.

$$H_I = \sum_{j=1}^{N-1} n_j n_{j+1}. \quad (32)$$

Using numerical exact diagonalization with periodic boundary conditions, we calculated the fidelity susceptibility for a system of 10 sites. The result is shown in Fig. 12 as a function of  $U$  and  $V$ . From the contour, one can clearly see the transition line for the PS-SDW, PS-CDW, CDW-SDW transitions, and the cross-over line in the PS phase. The fidelity susceptibility even shows a stronger peak around these boundaries than that in the  $U$ -driven case. As expected, it is a path-dependent quantity and we may also argue that the  $V$ -driven one is a more sensitive seeker to the continuous and the discontinuous phase transition in the extended Hubbard model than the  $V$ -driven one.

To have a finer structure of the phase boundaries, we chose two particular paths to study the fidelity susceptibility. The first one is along the  $U = 2$  line. The system goes through the PS, TS, SDW, BOW, and CDW phases when  $V$  increases from a very negative value. The other path is along the  $U = -2$  line. In this case, the system goes through the PS, SS, and CDW phases as  $V$  increases.



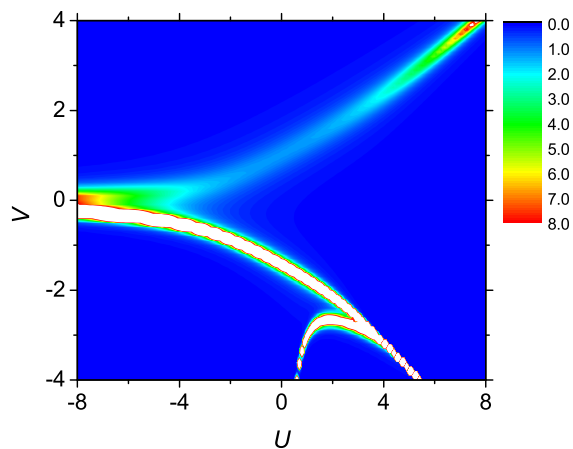
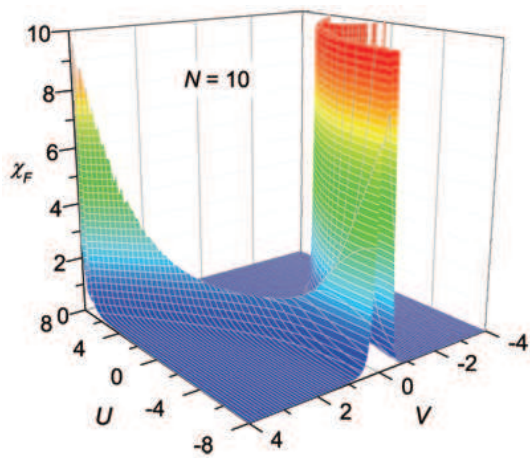


FIG. 12: (Top) A 3D plot of the fidelity susceptibility as a function of  $U$  and  $V$  in the 1D extended Hubbard model. (Bottom) A contour of the 3D plot on the  $U$ - $V$  plane.  $V$  is treated as the driving parameter in this case. The data is obtained from numerical exact diagonalization for  $N = 10$  with periodic boundary conditions.

### 1. Case I: $U = 2$

In Fig. 13, the fidelity susceptibility is plotted as a function of  $V$  for various system sizes. For  $V$  smaller than the range of value shown, the fidelity susceptibility is fluctuating with strong amplitudes. The change from the fluctuating pattern into a smooth one indicates roughly the boundary of the PS phase. Around the region of  $V = -1.3$ , the fidelity susceptibility has a point of inflection for  $N \geq 30$ . We expect that somewhere in this region, the fidelity susceptibility will develop a peak for large enough system and thus indicates a TS-SDW phase transition. However, we are not able to observe this with our current computational power.

Around  $V = 1.5$ , the fidelity susceptibility show a local maximum with non-trivial size dependence. As the system size increases, the amplitude of this local maximum

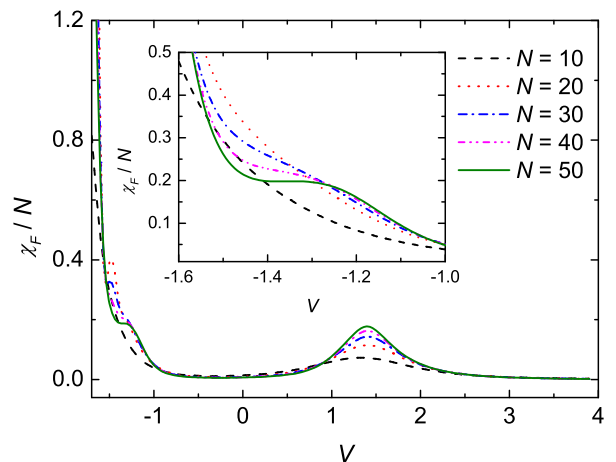


FIG. 13: A plot of the normalized fidelity susceptibility as a function of  $V$  in the 1D extended Hubbard model. Here  $U = 2$ . The inset shows a close-up of the fidelity susceptibility around  $V = -1.3$ .

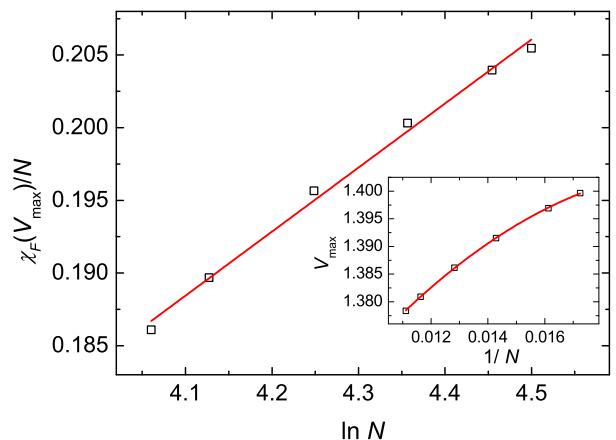


FIG. 14: A plot of the maximum of the fidelity susceptibility around  $V = 1.5$  as a function of  $\ln N$  in the 1D extended Hubbard model. Here  $U = 2$ . The straight line shows the linear fitting of the data points. The inset shows the scaling behavior of  $V_{\max}$  as a function of  $1/N$ . The curve is a second order polynomial fitting of the data.

also increases. From Fig. 14, we found that

$$\frac{\chi_F(V_{\max})}{N} \sim \ln N. \quad (33)$$

The nearest-neighbor interaction strength at which the local maximum take place, i.e.  $V_{\max}$ , is also plotted as a function of  $1/N$  in the inset of Fig. 14. From the second order polynomial fitting, we obtained

$$\lim_{N \rightarrow \infty} V_{\max} = 1.296 \pm 0.002. \quad (34)$$

In the thermodynamic limit, the fidelity susceptibility diverges and signals for a SDW-CDW phase transition.

However, for the transition into the BOW phase, we

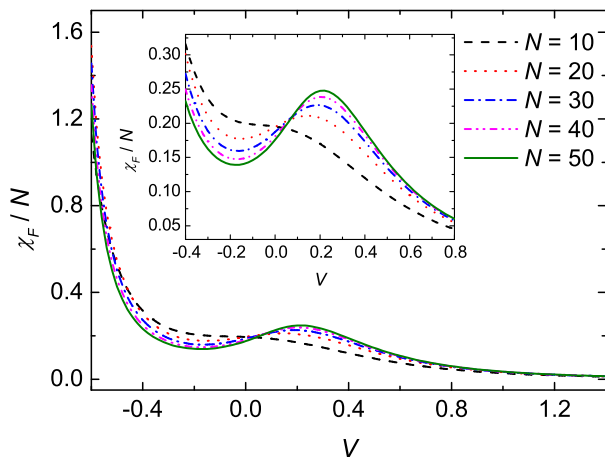


FIG. 15: A plot of the fidelity susceptibility as a function of  $V$  at  $U = -2$  in the 1D extended Hubbard model. The inset shows a close-up around  $V = 0.2$ .

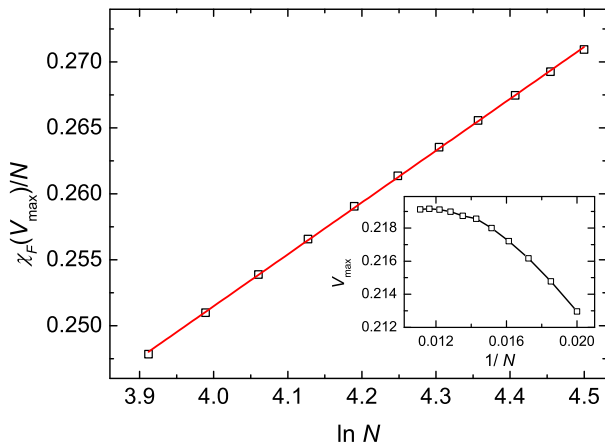


FIG. 16: A semi-ln plot of the maximum of fidelity susceptibility around  $V = 0.2$  versus  $N$  in the 1D extended Hubbard model. Here  $U = -2$ . The straight line shows a linear fitting of the data points. The inset shows a plot of  $V_{\max}$  as a function of  $1/N$ .

does not observe any significant signature in the fidelity susceptibility in this case.

## 2. Case II: $U = -2$

Figure 15 shows a plot of  $\chi_F/N$  as a function of  $V$  for  $U = -2$  in the system for various  $N$ . Again in the vicinity of the PS-SS phase transition around  $V = -0.6$ , the amplitude of the fidelity susceptibility shows a different pattern on the PS side to the SS side. Around  $V = 0.2$ , the fidelity susceptibility exhibits a local maximum. The magnitude of the maximum increases as the system size

increases. From the semi-ln plot in Fig. 16, we found that

$$\frac{\chi_F(V_{\max})}{N} \sim \ln N, \quad (35)$$

and it diverges logarithmically in the thermodynamic limit. This indicates a phase transition between the SS and CDW phase.

In the inset of Fig. 16, the  $V_{\max}$  around  $V = 0.2$  is shown as a function of  $1/N$ . The location of  $V_{\max}$  increases initially with the system size, but the rate of increase slows down as the system size increases. When reaching the maximum stimulated size  $N = 90$ , the value of  $V_{\max}$  shows a small drop compare with the one for  $N = 86$ . For the system size stimulated, we highly suspect that we still have not entered the scaling region and we would expect  $V_{\max}$  to decrease further as we increase the system size. A satisfactory scaling analysis on  $V_{\max}$  is not possible with our current computational power in this case.

## V. CONCLUSION

To conclude, we have investigated the fidelity susceptibility in the 1D Hubbard model and the extended Hubbard model. In the Hubbard model, we argued that the fidelity susceptibility diverges at two points infinitesimally close to the critical point while it remains extensive exactly at the critical point.

For the extended Hubbard model, we studied the fidelity susceptibility for the U-driven and V-driven cases. From the divergence of the fidelity susceptibility, one may notice the existence of the transition between PS-superconducting, superconducting-CDW, CDW-SDW, SDW-PS phases. Moreover, for the U-driven case, evidence for the CDW-BOW and BOW-SDW phase transition along  $V = 1$  was also found. However, in most of the above case, the critical points of the phase transition obtained from the scaling analysis showed discrepancies from previous studies (For examples in Ref. [49], [48], [50]). One of the reasons for the discrepancy may due to the limitation of system size being simulated. Another reason may due to the behavior of the fidelity susceptibility in an order-to-order phase transition. Like in the Hubbard model, the divergence in the fidelity susceptibility may not occurs exactly at the critical point. Similar founding was also obtained in the 1D Bose-Hubbard model in recent studies [55, 56]. The physical reason behind still require further studies.

W. C. Yu thank Wen-Long You for helpful discussion. This work is supported by the Earmarked Grant Research from the Research Grants Council of HKSAR, China (Project No. CUHK 401212).

- 
- [1] S. Sachdev, *Quantum phase transitions* (Cambridge University Press, Cambridge, England, 1999).
- [2] H. T. Quan, Z. Song, X. F. Liu, P. Zanardi, and C. Sun, *Phys. Rev. Lett.* **96**, 140604 (2006).
- [3] P. Zanardi and N. Paunković, *Phys. Rev. E* **74**, 031123 (2006).
- [4] P. Zanardi, M. Cozzini, and P. Giorda, *J. Stat. Mech.: Theory Exp.* **2007**, L02002 (2007).
- [5] M. Cozzini, P. Giorda, and P. Zanardi, *Phys. Rev. B* **75**, 014439 (2007).
- [6] P. Buonsante and A. Vezzani, *Phys. Rev. Lett.* **98**, 110601 (2007).
- [7] N. Oelkers and J. Links, *Phys. Rev. B* **75**, 115119 (2007).
- [8] S.-J. Gu, *Int. J. Mod. Phys. B* **24**, 4371 (2010).
- [9] W.-L. You, Y.-W. Li, and S.-J. Gu, *Phys. Rev. E* **76**, 022101 (2007).
- [10] P. Zanardi, P. Giorda, and M. Cozzini, *Phys. Rev. Lett.* **99**, 100603 (2007).
- [11] L. Campos Venuti and P. Zanardi, *Phys. Rev. Lett.* **99**, 095701 (2007).
- [12] S.-J. Gu, H.-M. Kwok, W.-Q. Ning, and H.-Q. Lin, *Phys. Rev. B* **77**, 245109 (2008).
- [13] S. Yang, S.-J. Gu, C.-P. Sun, and H.-Q. Lin, *Phys. Rev. A* **78**, 012304 (2008).
- [14] S.-J. Gu and W. C. Yu, arXiv:1408.2199 (2014).
- [15] V. L. Beresinskii, *Sov. Phys. JETP* **32**, 493 (1971).
- [16] J. M. Kosterlitz and D. J. Thouless, *J. Phys. C* **6**, 1181 (1973).
- [17] J. M. Kosterlitz, *J. Phys. C* **7**, 1046 (1974).
- [18] M.-F. Yang, *Phys. Rev. B* **76**, 180403 (2007).
- [19] J. O. Fjærestad, *J. Stat. Mech.: Theory Exp.* **2008**, P07011 (2008).
- [20] B. Wang, M. Feng, and Z.-Q. Chen, *Phys. Rev. A* **81**, 064301 (2010).
- [21] L. Campos Venuti, M. Cozzini, P. Buonsante, F. Massel, N. Bray-Ali, and P. Zanardi, *Phys. Rev. B* **78**, 115410 (2008).
- [22] M. Nakamura, *Phys. Rev. B* **61**, 16377 (2000).
- [23] E. Jeckelmann, *Phys. Rev. Lett.* **89**, 236401(2002).
- [24] E. Jeckelmann, *Phys. Rev. Lett.* **91**, 089702 (2003).
- [25] S. Chen, L. Wang, Y. Hao, and Y. Wang, *Phys. Rev. A* **77**, 032111 (2008).
- [26] M. C. Gutzwiller, *Phys. Rev. Lett.* **10**, 159 (1963).
- [27] J. Kanamori, *Prog. Theor. Phys.* **30**, 275 (1963).
- [28] J. Hubbard, *Proc. R. Soc. A* **276**, 238 (1963).
- [29] J. Hubbard, *Proc. R. Soc. A* **277**, 237 (1964).
- [30] J. Hubbard, *Proc. R. Soc. A* **281**, 401 (1964).
- [31] J. Hubbard, *Proc. R. Soc. A* **285**, 542 (1965).
- [32] J. Hubbard, *Proc. R. Soc. A* **296**, 100 (1967).
- [33] J. Hubbard, *Proc. R. Soc. A* **296**, 82 (1967).
- [34] R. Jördens, N. Strohmaier, K. Günter, H. Moritz, and T. Esslinger, *Nature* **455**, 204 (2008).
- [35] U. Schneider, L. Hackermüller, S. Will, T. Best, I. Bloch, T. Costi, R. Helmes, D. Rasch, and A. Rosch, *Science* **322**, 1520 (2008).
- [36] J. P. Farges, *Organic conductors* (Dekker, 1994).
- [37] R. Claessen, M. Sing, U. Schwingenschlögl, P. Blaha, M. Dressel, and C. S. Jacobsen, *Phys. Rev. Lett.* **88**, 096402 (2002).
- [38] D. Baeriswyl and H. Kiess, *Conjugated conducting polymers* (Springer, 1992).
- [39] V. J. Emery, *Phys. Rev. B* **14**, 2989 (1976).
- [40] M. Fowler, *Phys. Rev. B* **17**, 2989 (1978).
- [41] P. G. J. van Dongen, *Phys. Rev. B* **49**, 7904 (1994).
- [42] V. Emery, *Highly conducting one-dimensional solids* (Plenum, New York, 1979).
- [43] J. Sólyom, *Adv. Phys.* **28**, 201 (1979).
- [44] B. Fourcade and G. Sproken, *Phys. Rev. B* **29**, 5089 (1984).
- [45] J. Cannon and E. Fradkin, *Phys. Rev. B* **41**, 9435 (1990).
- [46] J. Voit, *Phys. Rev. B* **45**, 4027 (1992).
- [47] P. Sengupta, A. W. Sandvik, and D. K. Campbell, *Phys. Rev. B* **65**, 155113 (2002).
- [48] A. W. Sandvik, L. Balents, and D. K. Campbell, *Phys. Rev. Lett.* **92**, 236401 (2004).
- [49] Y. Z. Zhang, *Phys. Rev. Lett.* **92**, 246404 (2004).
- [50] S. Ejima and S. Nishimoto, *Phys. Rev. Lett.* **99**, 216403 (2007).
- [51] M. Tsuchiizu and A. Furusaki, *Phys. Rev. Lett.* **88**, 056402 (2002).
- [52] M. Tsuchiizu and A. Furusaki, *Phys. Rev. B* **69**, 035103 (2004).
- [53] C. Mund, O. Legeza, and R. M. Noack, *Phys. Rev. B* **79**, 245130 (2009).
- [54] G.-H. Liu and C.-H. Wang, *Commun. Theor. Phys.* **55**, 702 (2011).
- [55] J. Carrasquilla, S. R. Manmana, and M. Rigol, *Phys. Rev. A* **87**, 043606 (2013).
- [56] M. Łacki, B. Damski, and J. Zakrzewski, *Phys. Rev. A* **89**, 033625 (2014).